



14TH CANADIAN MASONRY SYMPOSIUM
MONTREAL, CANADA
MAY 16TH – MAY 20TH, 2021



DYNAMIC THERMAL PERFORMANCE OF COMMERCIAL WALL SYSTEMS

Huygen, Nathaniel¹ and Sanders, John²

ABSTRACT

Wall systems that have significant thermal mass show reduced energy usage compared to lightweight walls with a similar thermal resistance. Utilizing a specialized hot box apparatus, several wall systems were measured for both steady-state and dynamic thermal performance. Two types of wall systems were analyzed—the first consisted of a 2x6 steel-stud wall with various configurations of continuous insulation, batt insulation, and two different claddings—modular brick veneer or Exterior Insulation and Finish Systems (EIFS). The second type of wall consisted of an 8-inch lightweight concrete masonry unit (CMU), continuous insulation, and either modular brick veneer or EIFS cladding. A 24-hour day-night or “Sol-Air” cycle was imposed on the exterior of the assembly, and the total energy transfer through the wall measured. By utilizing a series of heat flux transducers in the hot box apparatus, localized performance in the zone of the steel-studs or CMU webs could be monitored during testing. Inclusion of modular brick veneer and an air cavity was found to improve the steady-state thermal resistance on average by 0.32 m²K/W and reduce the heat flow through the wall under the applied cycle by more than 30%. Experimental results were used to validate finite element modeling of these wall assemblies under steady-state and dynamic conditions. From these finite element models, the magnitude of the thermal bridging caused by the steel-studs could be quantitatively analyzed and a thermal framing factor calculated. Qualitative effects from thermal bridging of the steel-studs were obtained using an IR camera mounted within the metering chamber of the hot box apparatus.

KEYWORDS: *brick veneer, dynamic thermal performance, hot box apparatus, finite element modeling, IR camera*

¹ Research Associate, National Brick Research Center, 100 Clemson Research Blvd. Anderson, SC 29625, United States, nhuygen@clemson.edu

² Director, National Brick Research Center, 100 Clemson Research Blvd. Anderson, SC 29625, United States, jpsand@clemson.edu

INTRODUCTION

Evaluating the thermal performance of wall-systems is an important step in ensuring that the actual performance of the wall system meets the designed level of performance. Unfortunately, the only method to test these systems is a time consuming and expensive hot box test. Although steady-state component data can be measured using a heat flow meter apparatus conforming to ASTM C518, this does not give information about how the whole system performs. In addition, components containing thermal bridges “may yield very unreliable results” [1].

One of the drawbacks of ASTM C518, and other methods for measuring the thermal resistance, is that they do not account for the potential benefit of the thermal mass of the system. Under a dynamic thermal load, the thermal mass in the system serves to dampen the response of the system. The more thermal mass, the longer it takes the system to respond to the applied temperature. Previous studies of residential wall systems have demonstrated the benefit of thermal mass when the system is subjected to a dynamic thermal load [2, 3]. The addition of brick veneer to a two-by-four stud wall was found to reduce the energy transfer under the applied cycle by approximately 50% [2, 3].

Although there are several studies that discuss hot box results of residential wood-stud construction [2, 3, 4], there is very little testing data on typical commercial steel-stud walls. There is, however, data on commercial concrete and CMU walls available [5]. The prior hot box results from Van Geem [3, 5] also measured the dynamic performance under an applied temperature cycle. This cycle is referred to as the National Bureau of Standards (NBS) Sol-Air Cycle [6]. This is a 24-hour cycle designed to mimic the effect of convection and solar radiation on the wall temperature. This cycle has been adopted as a standard dynamic testing cycle so results between walls can be compared.

EXPERIMENTAL

Two types of wall systems were constructed and evaluated in the most recent round of testing. These consisted of eight steel-stud framed walls, and four CMU backed walls. These types of wall systems show very different behaviors due to the amount and placement of thermal mass within the system. The construction details of these wall systems are given in Table 1.

Each of the wall systems was tested for both steady-state and dynamic thermal performance. Steady-state thermal resistance was measured at four different mean temperatures to determine the average thermal resistance as well as its dependence on temperature. Although steady-state performance is a simple metric for comparing wall systems, it does not accurately portray the realistic performance of wall systems with significant thermal mass.

Table 1: Wall System Construction Details

Name	Cladding	Air Cavity	Continuous Insulation	Sheathing	Backup Wall	Interior
Steel-stud Wall	None	None	None	5/8" Fiberglass Faced Drywall	18-gauge 2x6 Steel-stud + R-21	5/8" Drywall
Steel-stud Wall with Continuous Insulation	None	None	2" XPS	5/8" Fiberglass Faced Drywall	18-gauge 2x6 Steel-stud + R21	5/8" Drywall
Steel-stud Wall with Continuous Insulation and no Batt Insulation	None	None	2" XPS	5/8" Fiberglass Faced Drywall	18-gauge 2x6 Steel-stud	5/8" Drywall
Brick Veneer over Steel-studs	Modular Brick Veneer	2"	None	5/8" Fiberglass Faced Drywall	18-gauge 2x6 Steel-stud + R21	5/8" Drywall
Brick Veneer over Steel-studs with Continuous Insulation	Modular Brick Veneer	1"	2" XPS	5/8" Fiberglass Faced Drywall	18-gauge 2x6 Steel-stud + R-21	5/8" Drywall
Brick Veneer over Steel-studs with Continuous Insulation and no Batt Insulation	Modular Brick Veneer	1"	2" XPS	5/8" Fiberglass Faced Drywall	18-gauge 2x6 Steel-stud + R21	5/8" Drywall
EIFS over Steel-studs	Stucco Skim Coat	None	2" EPS	5/8" Fiberglass Faced Drywall	18-gauge 2x6 Steel-stud + R21	5/8" Drywall
EIFS over Steel-studs and no Batt Insulation	Stucco Skim Coat	None	2" EPS	5/8" Fiberglass Faced Drywall	18-gauge 2x6 Steel-stud + R21	5/8" Drywall
Lightweight CMU Wall	None	None	None	None	8" Lightweight CMU	None
Lightweight CMU Wall with Continuous Insulation	None	None	2" XPS	None	8" Lightweight CMU	None
Brick Veneer over Lightweight CMU with Continuous Insulation	Modular Brick Veneer	None	2" XPS	None	8" Lightweight CMU	None
EIFS over Lightweight CMU	Stucco Skim Coat	None	2" EPS	None	8" Lightweight CMU	None

To measure the dynamic thermal performance, the interior temperature of the wall system was held constant at 24 °C (75.2 °F) while the exterior was subject to a 24-hour temperature cycle designed to mimic the combined effect of convection and solar radiation on the wall surface. The dynamic thermal performance was quantified by the total amount of energy transfer on the interior surface of the wall during the 24-hour cycle. This represents the combined heating and cooling load on a buildings HVAC system. The presence of thermal mass within the wall assembly resulted in a dampened response when compared to a light-weight wall assembly such as EIFS.

For the steel-stud wall systems, three walls were tested with brick veneer and different configurations of insulation in the backup wall. The walls were also tested without the brick veneer to determine how much the veneer contributed to the overall performance of the assembly. In addition, two EIFS wall systems were tested to compare different cladding materials. EIFS is a lightweight cladding made from polystyrene insulation with a stucco coat on the exterior. Similarly, the walls built with CMUs were also tested with and without brick veneer to determine how much the cladding impacted the overall performance.

Following experimental testing, finite element modeling was carried out in order to determine how significant an impact thermal bridging of the steel-studs was within the wall assembly. A two-dimensional finite element model was employed to calculate the thermal framing factor of each wall assembly.

The thermal framing factor gives the weight of the stud and insulation R-values in the calculation of the whole-wall thermal resistance [7]. The equation for calculating this resistance is given below:

$$\frac{1}{R_{avg}} = \frac{1-f}{R_{ins}} + \frac{f}{R_{stud}} \quad (1)$$

Where R_{avg} , R_{ins} , and R_{stud} are the thermal resistances of the whole-wall, insulation, and stud respectively. In a parallel thermal resistance calculation, the thermal framing factor (f) must be used instead of the cross-sectional area because of two-dimensional heat transfer effects caused by the difference in thermal conductivity between the stud and insulation. The greater the thermal framing factor, the more significant the thermal bridge for a given cross-sectional area.

The finite element results were qualitatively compared against an IR camera that was installed in the interior of the hot box apparatus that recorded images throughout the hot box testing. The magnitude of thermal bridging was readily evident in the difference in temperature between the insulation and stud temperatures visible on the interior wall surface. In the locations where thermal bridging occurred, the surface temperature over the steel-studs was closer to that of the exterior temperature.

RESULTS AND DISCUSSION

The presence of the steel-studs within the wall was found to have a large detrimental impact on the overall thermal performance of the wall system. The R-21 batt insulation was included in each stud wall, but whole wall thermal resistance was found to be only R-9.4. Adding two inches of continuous insulation to the wall resulted in the expected increase in thermal resistance of R-10. This was because the continuous insulation is not bypassed by steel framing members. The R-values of each wall assembly are reported in Table 2.

The dynamic thermal performance was found to vary significantly between the different wall systems. As expected, as the thermal resistance of the wall system increased, there was a

corresponding decrease in the dynamic energy transfer. There was also a significant reduction in energy transfer for the wall systems that contained thermal mass. The dynamic thermal performance results are also reported in Table 2.

Table 2: Measured Thermal Resistance and Dynamic Energy Transfer

Wall System	R-value [m ² K/W] (ft ² ·°F·hr/BTU)	Dynamic Energy Transfer [W·hr/m ² ·day] (BTU/ft ² ·day)
Steel-stud Wall	1.66 (9.4)	124 (39.3)
Steel-stud Wall with Continuous Insulation	3.56 (20.2)	46.4 (14.7)
Steel-stud Wall with Continuous Insulation and no Batt Insulation	1.82 (10.4)	104.5 (33.1)
Brick Veneer over Steel-studs	2.10 (11.9)	62.2 (19.7)
Brick Veneer over Steel-studs with Continuous Insulation	3.68 (20.9)	26.7 (8.5)
Brick Veneer over Steel-studs with Continuous Insulation and no Batt Insulation	2.08 (11.8)	60.9 (19.3)
EIFS over Steel-studs	3.29 (18.7)	51.1 (16.2)
EIFS over Steel-studs and no Batt Insulation	1.48 (8.4)	127 (40.3)
Lightweight CMU Wall	0.22 (1.3)	423 (134)
Lightweight CMU Wall with Continuous Insulation	1.67 (9.5)	62.6 (19.8)
Brick Veneer over Lightweight CMU with Continuous Insulation	1.80 (10.2)	36.4 (11.5)
EIFS over Lightweight CMU	1.38 (7.8)	67.8 (21.5)

The inclusion of the brick veneer over the steel-stud wall resulted in an average increase in thermal resistance of R-1.55 ft²·°F·hr/BTU (14.7%), while resulting in a decrease in energy transfer of 30.7%. This reduction in energy transfer by the brick veneer is shown graphically in Figures 1 and 2. The thermal mass helps to dampen the applied temperature cycle, reducing the temperature swing the rest of the wall experiences. The CMU walls showed a significantly reduced energy usage compared to the steel-stud walls for similar levels of thermal resistance. The reason for this was due to the placement of the thermal mass within the wall assembly. The benefit of thermal mass is greater when it is placed on the interior side of the insulation in the wall assembly.

In addition to decreasing the total energy transfer, the thermal mass had an additional benefit of delaying the time at which the peak energy usage occurs. The time at which peak energy usage occurred can be delayed by several hours when brick veneer is present. This time can be extended significantly if both brick veneer and CMUs are used in the wall assembly. Surprisingly, not only the thermal mass, but also the thermal resistance of the wall also had an impact on the time at which peak energy usage occurred. The difference between maximum applied temperature and the

maximum measured energy transfer is termed the lag time of the wall system. The lag time range from a low of one hour for the steel-stud wall, to a maximum of 8.8 hours for the brick veneer over lightweight CMU with continuous insulation. With the applied maximum temperature occurring roughly at 12:30 PM, this implies that the maximum energy usage for this wall would not be until almost 9:30 PM, well into the night. The dynamic energy transfer of the steel-stud walls and CMU walls is shown in Figure 1 and 2, respectively.

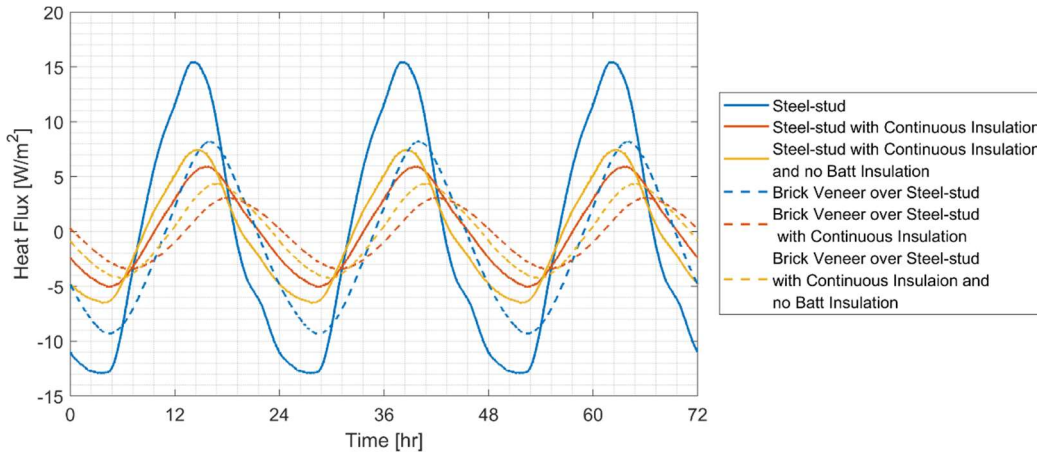


Figure 1: Dynamic Energy Transfer vs. Time for Steel-Stud Walls

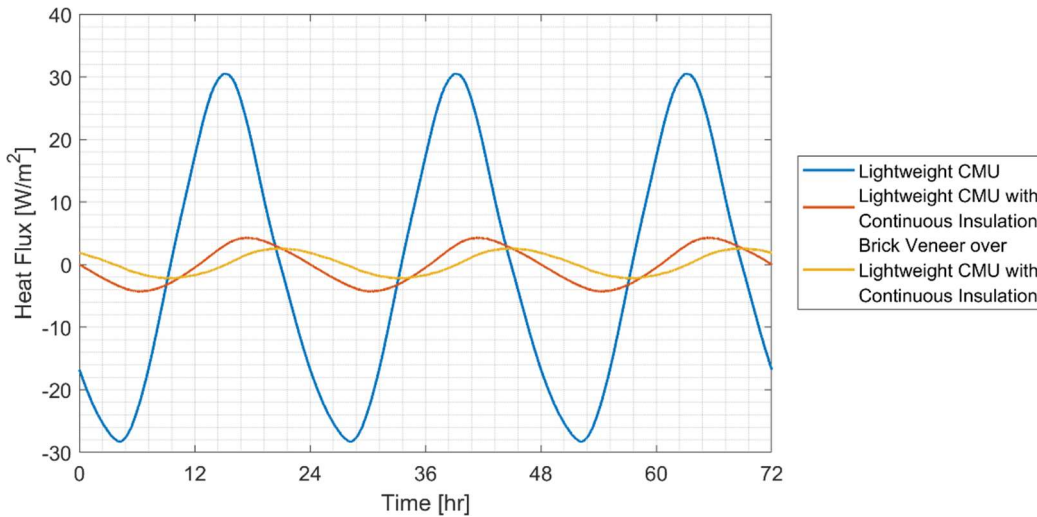


Figure 2: Dynamic Energy Transfer vs. Time for CMU Walls

Finite element modeling results were compared against those measured in the hot box apparatus to ensure the validity of the model. There was found to be excellent agreement between experimental and modeling results, well within the experimental error of the hot box apparatus for most wall assemblies. The experimental uncertainty of the hot box test was 12.4%. These results are reported in Table 3. The steel-stud wall with continuous insulation and no batt insulation, the lightweight CMU with continuous insulation, and the brick veneer over lightweight CMU with continuous insulation walls had a measured thermal resistance below that of the modeled value

and outside the experimental error due to the presence of wall ties within the assembly that bypassed the continuous insulation. It should also be noted that the steel-stud wall with continuous insulation was still within experimental error even though it also had wall ties due to the large thermal resistance of the assembly. When the continuous insulation was the only source of thermal resistance in the assembly, the effect of wall ties was found to be more significant on the overall heat transfer.

Table 3: Measured and Modeled Thermal Resistance

Wall System	Measured R-value [m ² K/W] (ft ² ·°F·hr/BTU)	Modeled R-value [m ² K/W] (ft ² ·°F·hr/BTU)	Thermal Framing Factor [-]
Steel-stud Wall	1.66 (9.4)	1.92 (10.9)	0.146
Steel-stud Wall with Continuous Insulation	3.56 (20.2)	3.88 (22.0)	0.173
Steel-stud Wall with Continuous Insulation and no Batt Insulation	1.82 (10.4)	2.20 (12.5)	0.024
Brick Veneer over Steel-studs	2.10 (11.9)	2.15 (12.2)	0.175
Brick Veneer over Steel-studs with Continuous Insulation	3.68 (20.9)	4.21 (23.9)	0.176
Brick Veneer over Steel-studs with Continuous Insulation and no Batt Insulation	2.08 (11.8)	2.48 (14.1)	0.024
EIFS over Steel-studs	3.29 (18.7)	3.45 (19.6)	0.173
EIFS over Steel-studs and no Batt Insulation	1.48 (8.4)	1.72 (9.8)	0.025
Lightweight CMU Wall	0.22 (1.3)	0.26 (1.50)	N/A
Lightweight CMU Wall with Continuous Insulation	1.67 (9.5)	2.04 (11.60)	N/A
Brick Veneer over Lightweight CMU with Continuous Insulation	1.80 (10.2)	2.32 (13.2)	N/A
EIFS over Lightweight CMU	1.38 (7.8)	1.57 (8.9)	N/A

The finite element model clearly demonstrates the significance of the thermal bridging caused by the steel-studs. Although the steel-studs were only 18-gauge thick and have a small cross-section relative to the total wall cross-section, the high thermal conductivity of steel relative to the other materials in the wall system caused the temperature gradient within the stud to be very low. This in turn results in a local zone of higher heat flux on the exterior wall surface. Since the size of the steel-stud that the wall sheathing is anchored to is approximately 1.5-inches, it behaves more like a 1.5-inch solid piece of steel than an 18-gauge member. The important parameter is the projected area in the direction of heat flow. The thermal bridging caused by the steel-studs is shown in Figure 3. The two-dimension heat transfer that thermal bridging causes can be seen visually as a deflection in the temperature field from a linear gradient across the assembly. The steel-stud wall with

continuous insulation and no batt insulation did not have much thermal bridging whereas the steel-stud wall and the steel-stud wall with continuous insulation did have significant thermal bridging.

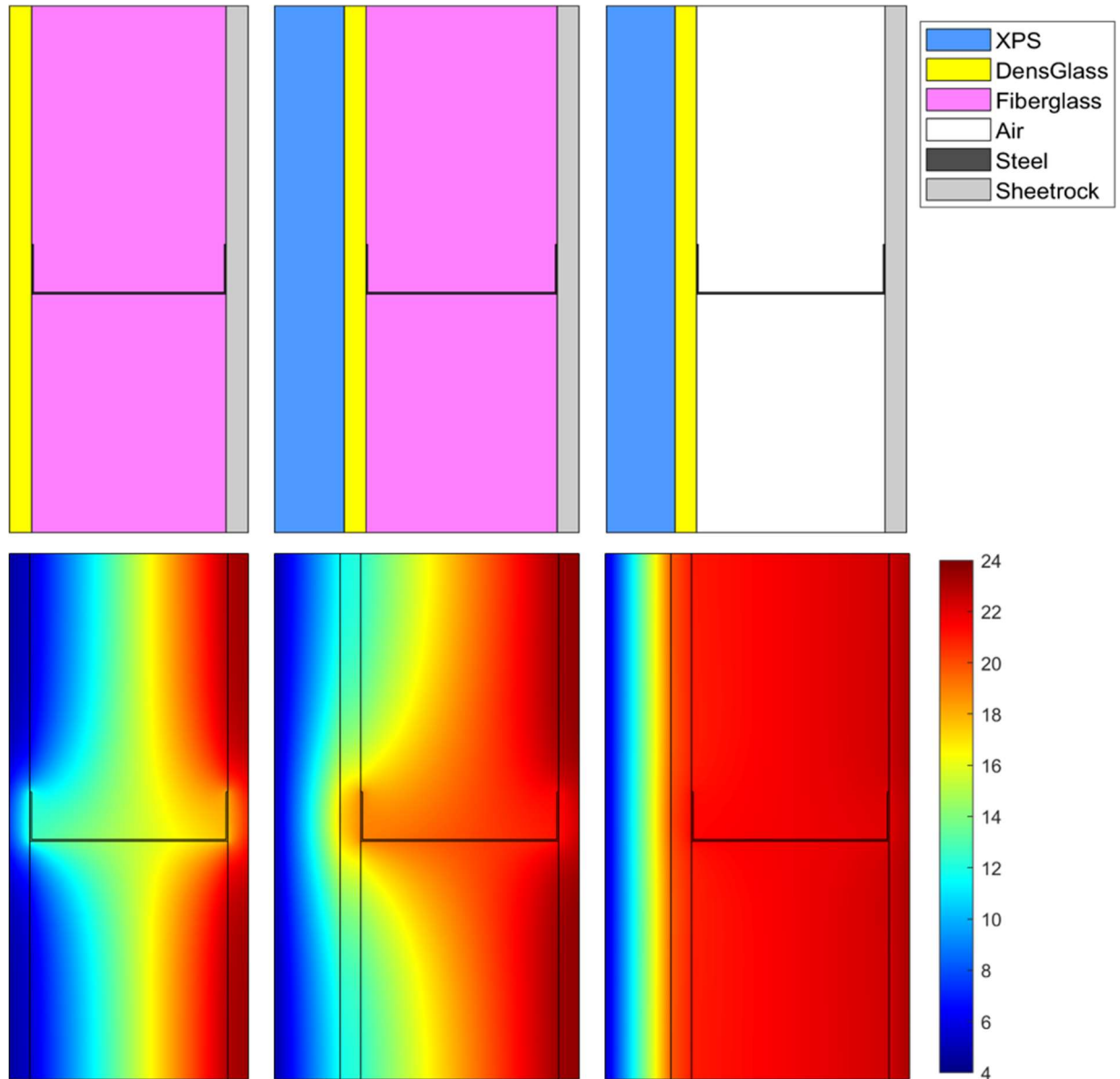


Figure 3: Finite Element Results Showing Thermal Bridging. Cross-Sectional View (top) and Temperature Field (bottom). Steel-Stud Wall (left), Steel-Stud Wall with Continuous Insulation (center), and Steel-Stud Wall with Continuous Insulation and no Batt Insulation (right).

In addition to finite element modeling, IR camera images taken from inside the hot box also demonstrated the thermal bridging of the steel-studs. The steel-studs allow a significantly more heat trough them than the insulation resulting in a significantly different temperature over the studs as compared to over the insulation which was clearly visible in the IR camera images. Interestingly, the framing factor was found to depend on the geometry of the wall as well as the thermal

resistance of the wall components. When continuous insulation was added to the assembly, the framing factor was found to decrease implying that the thermal bridging effect was being mitigated. This resulted in a greater than expected increase in the overall resistance of the wall system. When the walls without batt insulation were tested, there was found to be a drastic reduction in the framing factor. When the batt insulation was removed, the thermal resistance of the stud-wall cavity decreased sharply. This drop in thermal resistance was found to alter the amount of heat flowing through the studs from two-dimensional heat transfer. IR camera images from brick veneer walls one through three are shown in Figure 4.

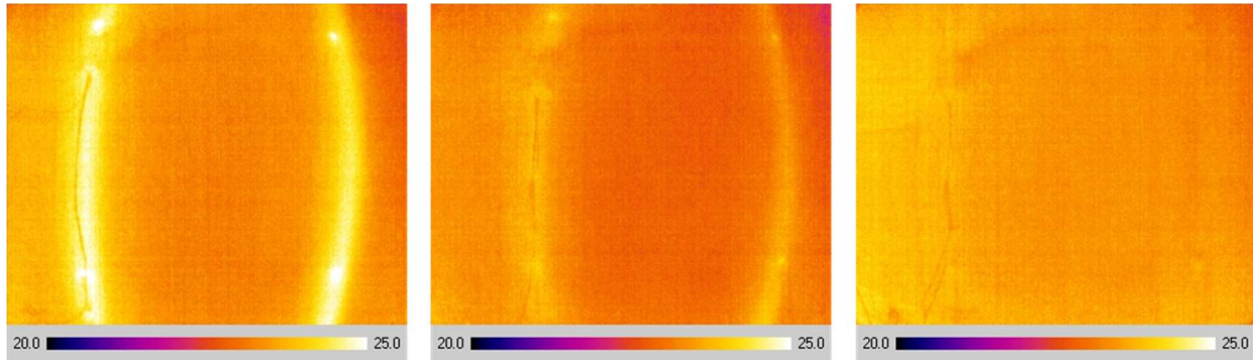


Figure 4: IR Camera Images of the Interior Surface of Brick Veneer over Steel-stud (left), Brick Veneer over Steel-stud with Continuous Insulation (center), and Brick Veneer over Steel-Stud with Continuous Insulation and no Batt Insulation (right).

Finite element modeling also allows for calculating how much the thermal mass reduced the overall heat transfer. It was found that even a lightweight wall system had some amount of thermal mass benefit. The benefit of the thermal mass was quantified by modeling the dynamic performance of the wall assembly both with and without mass, then calculating the ratio between the difference in energy to the energy transfer without mass. The wall was modeled without mass by setting the density of each component to zero. This represents the percent reduction in dynamic energy transfer directly attributable to the thermal mass of the system. These results are reported in Table 5. The benefit of the thermal mass was found to depend on the amount and placement of the insulation in the wall assembly.

Table 5: Reduction in Energy Transfer by Thermal Mass

Wall System	Dynamic Energy Transfer [Whr/m ² ·day] (BTU/ft ² ·day)	Dynamic Energy Transfer (no mass) [Whr/m ² ·day] (BTU/ft ² ·day)	Reduction
Steel-stud Wall	110 (34.9)	122 (38.7)	9.3%
Steel-stud Wall with Continuous Insulation	36.4 (11.5)	63.3 (20.1)	42.5%
Steel-stud Wall with Continuous Insulation and no Batt Insulation	89.4 (28.3)	107 (33.9)	16.6%
Brick Veneer over Steel-studs	49.5 (15.7)	109 (34.6)	54.4%
Brick Veneer over Steel-studs with Continuous Insulation	17.5 (5.5)	58.5 (18.5)	70.1%
Brick Veneer over Steel-studs with Continuous Insulation and no Batt Insulation	43.7 (13.9)	96.7 (30.7)	54.8%
EIFS over Steel-studs	43.4 (13.8)	70.8 (22.4)	38.6%
EIFS over Steel-studs and no Batt Insulation	111 (35.2)	133 (42.2)	16.1%
Lightweight CMU Wall	406 (128.7)	529 (167.7)	23.3%
Lightweight CMU Wall with Continuous Insulation	57.9 (18.4)	115 (36.5)	49.5%
Brick Veneer over Lightweight CMU with Continuous Insulation	28.7 (9.1)	105 (33.3)	72.6%
EIFS over Lightweight CMU	75 (23.8)	145 (46.0)	48.4%

CONCLUSION

Commercial wall systems containing steel-studs present a challenge in accurately measuring the thermal performance because of the significant amount of two-dimensional heat transfer. This two-dimensional heat transfer results in whole-wall performance significantly below that of the batt insulation in both steady-state as well as dynamic testing. Two-dimensional finite element modeling was able to accurately account for this thermal bridging and predict both the steady-state and dynamic thermal performance of the wall systems.

Wall systems that contained thermal mass, such as brick veneer or CMUs, showed enhanced thermal performance under dynamic conditions that was not represented by steady-state measurements. This thermal mass benefit was able to be quantitatively measured in a hot box apparatus by measuring the total energy transfer through the wall assembly during the applied temperature cycle. This benefit was further quantified by performing finite element modeling of the wall systems under the applied dynamic cycle with and without thermal mass and looking at the difference in energy usage.

Residential wall systems that contain wood-studs do not show the same amount of thermal bridging that commercial walls do due to the wood not being as good of a conductor of heat. The thermal mass benefit found for the brick veneer commercial walls was found to be similar to that of the brick veneer residential walls tested in the previous round of testing [2]. The largest impact on the thermal mass benefit from the cladding depends on the amount of thermal insulation and thermal mass of the backup wall.

IR cameras installed within the hot box apparatus proved to be an excellent tool for qualitatively analyzing the magnitude of the thermal bridging occurring within the steel-stud wall assemblies. The steel-studs were clearly visible within the infrared images due to them having a higher heat flow through them.

REFERENCES

- [1] ASTM International. *C518-17 Standard Test Method for Steady-State Thermal Transmission Properties by Means of the Heat Flow Meter Apparatus*. West Conshohocken, PA; ASTM International, 2017. <https://doi.org/10.1520/C0518-17>
- [2] N. Huygen and J. Sanders, "Dynamic Thermal Performance Measurements of Residential Wall Systems," in *Masonry 2018*, edited by Krogstad, N. and McGinley, W. (West Conshohocken, PA: ASTM International, 10.1520/STP161220170173), 106-2018. <https://doi.org/978-0-8031-7670-6>
- [3] M. G. Van Geem, "Calibrated Hot Bot Test Results Data Manual – Volume I," Construction Technology Laboratories, Skokie, Illinois, 1984.
- [4] N. Huygen and J. Sanders, "Dynamic Thermal Performance Measurements of Residential Wall Systems Part II, with Numerical Validation of Steady-State Performance," 13th North American Masonry Conference, 2019.
- [5] M. G. Van Geem, S. C. Larson, "Calibrated Hot Box Test Results Data Manual – Volume II," Construction Technology Laboratories, Skokie, Illinois, 1985
- [6] B. A. Peavy, F.J. Powell, D. M. Burch, "Dynamic Thermal Performance of an Experimental Masonry Building," National Bureau of Standards, Washington, D.C., 1973
- [7] J. Kosny, D. W. Yarbrough, P. Childs, "Effects of Framing on the Thermal Performance of Wood and Steel-Framed Walls," *Improving Building Systems in Hot and Humid Climates*, Orlando, FL, 2006.